

Optical and surface properties of hybrid TiO_2 /ormosil planar waveguide prepared by the sol–gel process

Baoling Wang^{*}, Lili Hu

Shanghai Institute of Optics and Fine Mechanics, Chinese Academy of Sciences, P.O. Box 800-211, Shanghai 201800, PR China

Received 13 January 2004; received in revised form 28 June 2004; accepted 18 November 2004

Available online 5 February 2005

Abstract

Two kinds of silanes, 3-glycidoxypolytrimethoxysilane (GLYMO) and 3-trimethoxysilylpropylmethacrylate (TMSPM), were used to prepare ormosil waveguide films by the sol–gel method. Thirty percent $\text{Ti}(\text{OBu})_4$ and 70% silane were contained in the precursor sols. The properties of films were measured by scanning electron microscopy (SEM), Fourier transform infrared spectroscopy (FTIR), UV/VIS/NIR spectrophotometer (UV–vis), atomic force microscopy (AFM), m-line and scattering-detection method. The films from GLYMO and TMSPM precursors exhibit similar thickness (2.58 μm for GLYMO, 2.51 μm for TMSPM) and refractive index (1.5438 for GLYMO, 1.5392 for TMSPM, $\lambda = 632.8 \text{ nm}$), but the film from TMSPM precursor has higher propagation loss (1.024 dB/cm, $\lambda = 632.8 \text{ nm}$) than the film prepared from GLYMO (0.569 dB/cm, $\lambda = 632.8 \text{ nm}$). Furthermore, the film prepared from TMSPM is easy to be opaque and cracks during coating whereas the same phenomenon was not found for the film prepared with GLYMO. It is confirmed that GLYMO is a better precursor than TMSPM for waveguide film preparation.

© 2005 Elsevier Ltd and Techna Group S.r.l. All rights reserved.

Keywords: C. Optical properties; Sol–gel waveguide

1. Introduction

Planar waveguides have recently been paid much attention due to their promising applications in integrated optics [1–5]. The formation of waveguide requires the guiding layer with refractive index higher than those of the substrate and cladding. The number of guiding mode depends on the thickness and refractive index of the guiding layer. In spite of the fact that pure inorganic films with low optical losses made by sol–gel technique combine good mechanical and thermal stability, crack-free and thicker ($d > 1 \mu\text{m}$) coatings are difficult to be obtained with only inorganic precursors. In fact, high treatment temperature is necessary to burn out organic components in films and then make films densification [6–9]. Organically modified silica (ormosil) materials derived from sol–gel process combine inorganic with organic properties, where inorganic ingredient is mainly responsible for adjusting the refractive index

and maintaining the hardness of films. Decreased network connectivity originated from organic component leads to an enhanced relaxation rate and to a lower densification temperature. Thus, crack-free and thicker films can be easily deposited in a single step by spin-coating or dip-coating method and the preparation of multimode waveguides become possible [10–11].

In recent years, investigations on inorganic–organic hybrid planar waveguides prepared by sol–gel route are gradually increasing due to their outstanding advantages compared with other methods. Many articles have stressed the selection of alkoxide, solvent, catalyst, organic precursors, and synthesis process, which really affect the optical properties of waveguide films through changing the microstructure such as porosity, cluster size, and surface roughness [12–15]. Ormosil materials containing TiO_2 , ZrO_2 , GeO_2 , PbO , and ZnO have been prepared by sol–gel method. Results indicated that planar waveguides with losses typically ranging from 0.25 to 4 dB/cm are possible to achieve [16]. However, little research has been carried out on the effect of different organic precursors on optical properties of films.

^{*} Corresponding author. Tel.: +86 21 5991 0994; fax: +86 21 3991 0393.

Atkins et al. [17] reported the effect of an ormosil system comprising methyl- and phenyl-substituted silica on the film optical properties, where methyl and phenyl play an opposite role in adjusting refractive index. However, they did not measure the propagation losses. 3-Glycidoxypropyltrimethoxysilane (GLYMO) and 3-(trimethoxysilil)propylmethacrylate (TMSPM) are typical chemicals often used as organic precursors. GLYMO is an epoxysilane, which can react by the formation of polyether linkages. These reactions can be catalyzed by the addition of amine compounds like in many conventional organic epoxide systems. TMSPM, instead, is a methacrylate alkoxy silane, which can react by radical polymerization or in combination with multifunctional amines by a covalent nucleophilic polyaddition type reaction. Both of them act as network formers in films [18]. In the present work, particular attention was paid to the effect of either GLYMO or TMSPM on the optical properties of waveguide films. In addition, the optical properties of films prepared by GLYMO with different heat treatment processes were also investigated in order to find proper firing condition.

2. Experimental

Two different silanes, 3-glycidoxypropyltrimethoxysilane [GLYMO > 98.8%] or 3-trimethoxysililpropylmethacrylate [TMSPM 95.4%], were used as organic precursors, titanium butoxide [$\text{Ti}(\text{OBu})_4$ > 98.0%] as inorganic precursor. The detailed procedure of sol synthesis is described as follows: GLYMO or TMSPM was dissolved in ethanol, and prehydrolyzed with H_2O (molar ratio GLYMO (or TMSPM): H_2O = 1:1). This solution was stirred for 1 h, then mixed with another solution, prepared by mixing Ti-alkoxide and acetylacetone (Acac) and stirring for about 15 min (molar ratio Ti:Acac = 1:1). The mixed solution was stirred for 2 h and the resultant sol was obtained (molar ratio $\text{Ti}(\text{OBu})_4$:GLYMO (or TMSPM) = 30:70). The final sols will be indicated as GT (GLYMO + $\text{Ti}(\text{OBu})_4$) and TT (TMSPM + $\text{Ti}(\text{OBu})_4$). All the experiments were performed at room temperature and atmosphere humidity (60%). It should be noted that HCl solution must be added to TT to ensure pH < 6 and therefore promote TMSPM hydrolyzing, otherwise phase separation would appear in the solution. All the films were obtained by dip-coating with the withdrawal speed of 1 cm/min. Soda-lime-silica glass slides and silicon wafers were used as substrates after ultrasonically cleaning with acetone, distilled water and ethanol. The viscosity of sols was measured at once after coating films. The prepared sols were stored in the darkness and aged for 1 week altogether. The coated films from GT sol were dried at room temperature or fired at 50, 100, 150, and 200 °C for different durations from 2 to 17 h. The films from TT sol were only fired at 150 °C for 2 h, or dried at room temperature.

The film thickness was measured with a scanning electron microscope (SEM) (JSM-6360LV). Fourier trans-

form infrared (FTIR) absorption spectrum of the film deposited on silicon wafer was determined by a FTIR spectrometer (NEXOS, Thermo Nicolet) in the range of 4000–400 cm^{-1} . The UV-vis transmittance spectrum of film deposited on soda-lime-silica glass slide in the range of 250–700 nm was examined by a 900UV/VIS/NIR spectrophotometer (Perkin-Elmer, Labmda). Surface morphology and the root mean square (rms) roughness of film were determined by atomic force microscopy (AFM) (Park Scientific Autoprobe CP). The scan area was 1 $\mu\text{m} \times 1 \mu\text{m}$. The refractive index of film was measured with dark m-line spectroscopy [19]. The incident light wavelength was $\lambda = 632.8 \text{ nm}$. The viscosity of sol was measured with rotation viscosimeter (NJD-1). The scattering-detection method was used for optical loss measurement of the film [20]. The laser light ($\lambda = 632.8 \text{ nm}$, He-Ne laser) was launched into the waveguide by a prism and the polarization of the laser beam was parallel to the plane of the waveguide (TE mode). The scattered light was collected in a direction perpendicular to the plane of the film, using a CCD camera and the loss was measured through an exponential fit of the decaying scattered intensity, assuming a homogeneous distribution of the scattering centers in the film.

3. Results and discussion

3.1. The effect of heat treatment on the film thickness and the refractive index

The thickness and refractive index of films prepared with GLYMO are shown in Fig. 1(a) and (b). All the films are single layer. Fig. 1(a) gives the change of thickness and refractive index of the films, which were coated on soda-lime-silica glasses and fired at different temperatures for 2 h. As expected, the film thickness decreases and the refractive index increases when the heat treatment temperature rises from room temperature to 200 °C, which is attributed to the condensation of film resulting from the removal of water and solvent in film. However, it deserves to note that the film without heat treatment is very soft and prone to be scratched even after storage for 1 week in air. Fig. 1(b) shows the dependence of the film thickness and refractive index on the firing time; all the samples were fired at 150 °C. It is clearly observed that the refractive index rises but thickness drops with the increasing heat treatment duration. Therefore, longer duration of thermal treatment is also beneficial to the removal of water and solvent and the densification of film. In order to demonstrate those conclusions, FTIR spectrometer was used to examine the structure change of the film in firing process.

3.2. The FTIR spectra of the films

Fig. 2(a) and (b) reports the FTIR absorption spectra of films prepared with GT sol in the range of 400–4000 cm^{-1} .

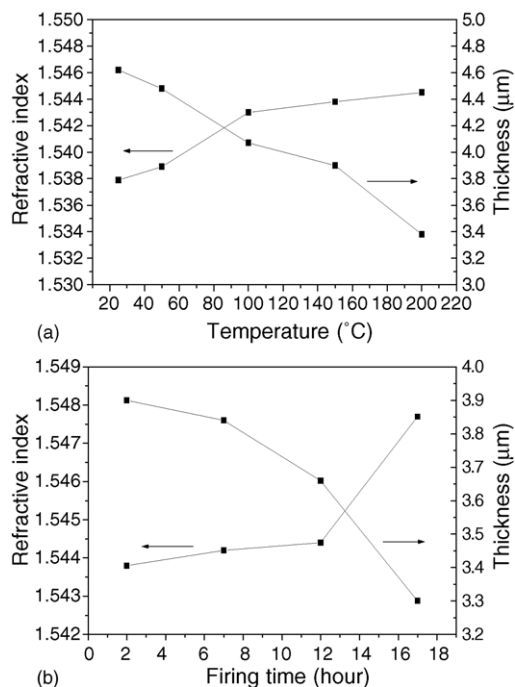


Fig. 1. Dependence of the thickness and refractive index of the GT films on (a) firing temperature, (b) firing time.

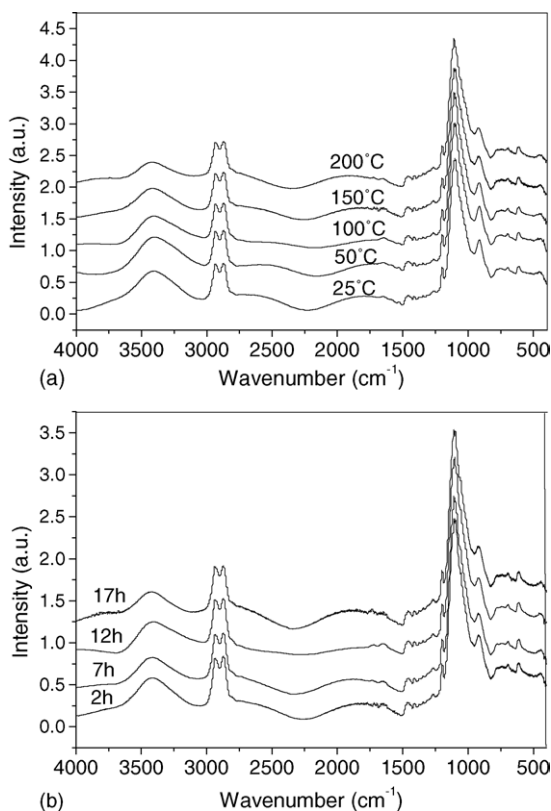


Fig. 2. FTIR absorption spectra of GT films fired at (a) different temperatures for 2 h, (b) 150 °C for different time.

The films were deposited on silicon wafers. Fig. 2(a) shows the absorption spectra of films dried at room temperature and fired at different temperatures of 50, 100, 150, and 200 °C for 2 h. Fig. 2(b) gives the absorption spectra of films fired at 150 °C. All spectra show an absorption band at 1100 cm⁻¹ due to Si–O–R stretching vibration of ethoxy groups directly bonded to silicon, which are overlapped to the Si–O–Si region around 1000–1200 cm⁻¹ [21]. The bands at 1190 cm⁻¹ are attributed to CH₃ rocking vibration [13]. The bands between 910 and 940 cm⁻¹ are assigned to Si–O–Ti stretching overlapped to residual Si–OH stretching vibrations and non-bridging oxygen Si–O⁻ [22]. Furthermore, there are broad peaks at 2892 cm⁻¹ due to –CH₂–symmetric stretching [13], another broad peaks between 3100 and 3500 cm⁻¹ correspond to OH stretching. The bands at around 620 cm⁻¹ are due to the silicon substrates. It can be observed that both higher temperature and longer heat-treatment time help to reduce band intensity of OH groups, but no obvious change with other band intensity is observed. It confirms that the water content in film decreases with increase of temperature and duration of thermal treatment.

Fig. 3 gives the FTIR absorption spectra of films prepared with TT sol. The films were deposited on silicon wafers fired at 150 °C for 2 h and dried at room temperature. Comparing with Fig. 2, a new band at 1658 cm⁻¹ is observed in Fig. 3. This band is considered to be the C=C stretching mode of the methacrylate groups of TMSPM. At the same time, the main difference between both TT films fired at 150 °C and dried at room temperature is the disappearance of C=O double band at 1729 cm⁻¹ in 150 °C fired film. This indicates that thermal treatment causes chemical reaction in the film from TT sol. The dependence of viscosity of both GT and TT sols upon aging time was examined and results are given in Fig. 4. The viscosity of GT sol changed quickly after aging for 1 week, whereas no variation was observed in TT sol. These facts can be attributed to the important structure difference between GLYMO and TMSPM. For GLYMO the formation of Si–O–Si network happens via the opening of the epoxy rings and the formation of a polyethylene oxide chain. The ring opening is achieved by using the titanium

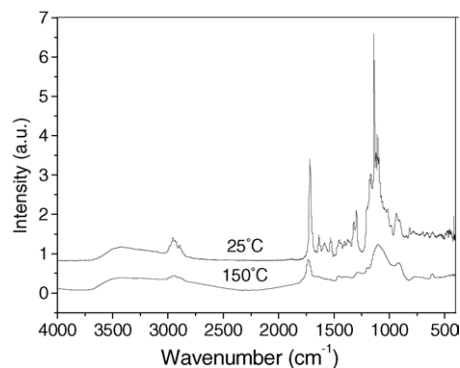


Fig. 3. FTIR absorption spectra of TT film fired at 150 °C for 2 h and dried at room temperature (25 °C).

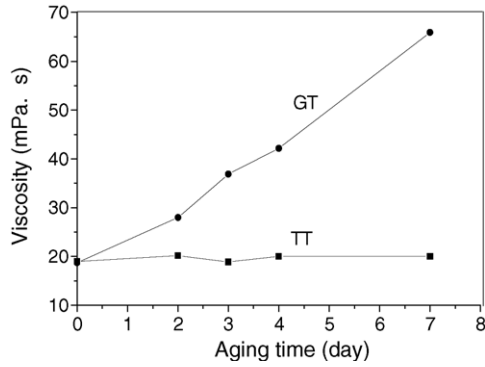


Fig. 4. Dependence of the viscosity of both sols upon aging time.

alkoxide as catalyst. $\text{Ti}(\text{OBU})_4$ plays a double role as a precursor for the inorganic oxide formation and catalyst for the organic polymerization in GLYMO [21]. The polymerization proceeds gradually in GT sol with aging. The thermal treatment of the deposited film does not affect the initial epoxy ring opening in GLYMO precursor [23]. However, polymerization of methacrylate groups of TMSPM precursor can be activated only by heating. The organic network chain is not formed during the sol aging process [21]. Thus, the viscosity does not increase during aging.

3.3. The UV–vis spectra of the films

The UV–vis transmittance spectra of two films prepared with GT and TT sols coated on soda-lime–silica glass slides are shown in Fig. 5. Both films are fired at 150 °C for 2 h. The GT film is not only transparent but also colorless. Instead, the TT film is transparent but yellow. It can be seen from Fig. 5 that both films exhibit sharp absorption edges and the maximum transmission exceeds 90%, which indicates that the films have no intrinsic absorption [24]. But it is evident that the transmittance of TT film is lower than that of GT film in the 300–550 nm wavelength range.

The optical absorption coefficient of films can be evaluated from transmittance [25]:

$$T = A \exp(-\alpha d) \quad (1)$$

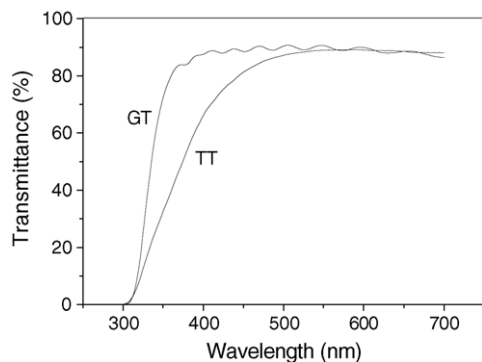


Fig. 5. UV–vis transmittance spectra of GT and TT films.

where T is transmittance, d is film thickness, A is a coefficient related to the refractive index, which is nearly equal to unity at the absorption edges, and α is the absorption coefficient. The band gap energy (E_g) of film can be estimated from the absorption coefficient by fitting the data to the relation [26]:

$$\alpha h\nu = B(h\nu - E_g)^n \quad (2)$$

where $h\nu$ is the incident photon energy, B the edge width parameter and n an exponent that determines the type of electronic transition causing the absorption, which is 1/2, 3/2, 2, 3 for direct allowed, direct forbidden, indirect allowed, and indirect transition, respectively. The transmittance data were found to fit $n = 3/2$, because the $(\alpha h\nu)^{2/3}$ versus $h\nu$ plots are linear in a certain range as seen in Fig. 6. It means that the type of electronics transition causing absorption is direct forbidden. The band gap energy E_g of the films can be obtained by extrapolating the linear region of the plot to 0. As can be seen from Fig. 6, the values of E_g are 3.78 and 3.62 eV for GT and TT films, respectively. Because the film was believed to consist of nanometric cluster of titania and exhibit quantum size effect, the following equation was used to calculate the size of titania clusters [27]:

$$E_g = E_b + \frac{\pi^2 \hbar^2}{2r^2} \left(\frac{1}{m_e^*} + \frac{1}{m_h^*} \right) - 1.8 \frac{e^2}{\epsilon r} \quad (3)$$

that is

$$E_g = E_b + \frac{2.45}{r^2(nm)} - \frac{0.45}{r(nm)} \quad (4)$$

where E_b is the band gap energy of bulk material, \hbar the Planck's constant, $m_{e,h}^*$ are effective masses of electrons and holes, respectively, ϵ and r are dielectric susceptibility and radius of TiO_2 clusters, respectively. The estimated radius of TiO_2 clusters is 1.70 and 1.94 nm for GT and TT films, respectively. Therefore, the relative lower transmittance of TT film may be ascribed to the bigger size of TiO_2 clusters, which is probably due to the hydrophobic nature of TMSPM that favors the aggregation of hydrophilic titania thermodynamically.

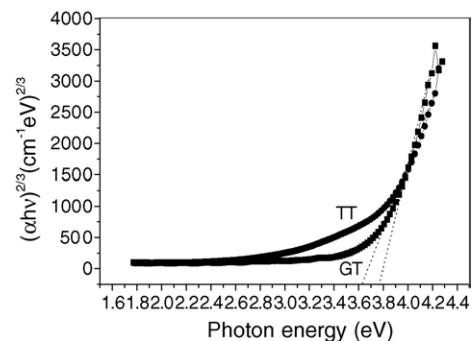


Fig. 6. Plots of $(\alpha h\nu)^n$ vs. photon energy of both GT and TT films.

Table 1

The properties of the films from GT and TT sols

| Sample | Thickness (μm) | Refractive index | Attenuation (dB/cm) |
|--------|-----------------------------|---------------------|---------------------|
| GT | 2.58 ± 0.01 | 1.5438 ± 0.0001 | 0.569 ± 0.001 |
| TT | 2.51 ± 0.01 | 1.5392 ± 0.0001 | 1.024 ± 0.001 |

The films were fired at 150°C for 2 h and the refractive index were measured at $\lambda = 632.8\text{ nm}$.

3.4. The optical properties of the films

The properties of films from GT and TT sols are shown in Table 1. These two kinds of films have similar thickness because of their similar viscosity as seen in Fig. 4. The refractive index of GT films is a little larger than that of TT films, indicating that the former has higher density. Moreover, the loss of GT films is 0.569 dB/cm , suggesting a high level of chemical homogeneity in this hybrid waveguide. In general, the more the number of constituents of a film, the higher the probability of high optical loss, since attenuation is directly related to refractive index fluctuations within the network [16]. AFM was used to examine the surface morphology and rms roughness of the films. Fig. 7 shows the surface morphologies of GT and TT films coated on soda-lime-silica glass slides. It can be seen that both films have dense and porous-free morphology and small roughness. In fact, the measured rms data are 0.192 and 0.328 nm for GT and TT films, respectively. Since the values are smaller than 1 nm , the waveguide optical losses significantly are not from the surface roughness [21]. But the loss of TT film is 1.024 dB/cm , relatively higher and beyond 1 dB/cm . This result is probably attributed to two aspects: firstly, in a multi-component system where the starting materials have different hydrolysis rates, the homogeneity of the resultant ormosil is an important consideration. For TT sol, the hydrolysis rate of TMSPM is very different from that of Ti-alkoxide, the former hydrolyzes with water only under acid condition, whereas Ti-alkoxide can hydrolyze with water rapidly. So the homogeneity of TT sol is problematic. It was found that the film from 4 days aged TT sol was easy to be opaque. After the TT sol aging for 7 days, the film was not only opaque but also cracked even without heat treatment, while the film from 1 week aged GT sol was still transparent and crack-free. Secondly, the non-homogeneous chemical reactions occurred in solid TT film during the thermal treatment as discussed in Section 3.2. As we know, the chemical reaction in liquid is always more homogeneous than that in solid. Therefore, the non-homogeneous chemical reactions lead to ununiformity of structure and followed by high loss. In fact, the refractive indices of different points of TT film are different, which demonstrates the non-homogeneity of hybrid film. Besides, the larger dimensions of TiO_2 clusters in TT film as discussed above are also the reasons of higher loss for TT film. Meanwhile, although the surface roughness of film is not a dominating aspect affecting attenuation,

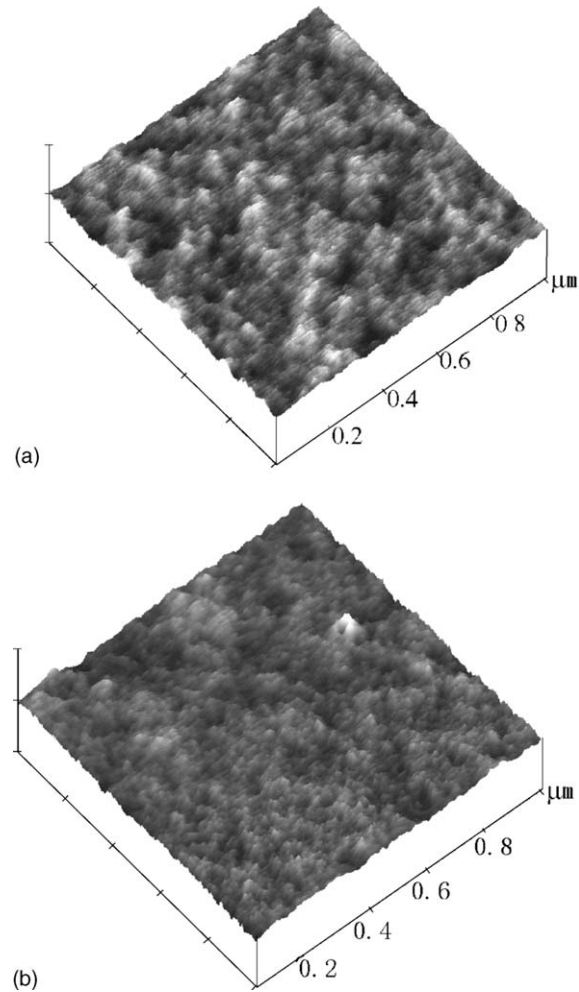


Fig. 7. AFM micrographs of (a) GT film, (b) TT film fired at 150°C for 2 h.

higher roughness of TT film can still produce larger light scattering. TT film, therefore, has higher attenuation than GT film.

4. Conclusions

Two kinds of hybrid inorganic–organic waveguide films prepared from $\text{Ti}(\text{OBu})_4$ + 3-glycidoxypolytrimethoxysilane (GLYMO) and $\text{Ti}(\text{OBu})_4$ + 3-trimethoxysilylpropylmethacrylate (TMSPM) sols have been fabricated by sol-gel process. It was found that a heat treatment temperature of 150°C for 2 h is appropriate to obtain low surface roughness and high transparency in the visible range for GT and TT films. There is no obvious difference in film thickness and refractive index between the two kinds of hybrid films. However, TMSPM is responsible for the high propagation loss of TT film, because chemical reactions occurred in solid TT film during heat treatment and different hydrolysis rates between TMSPM and Ti-alkoxide lead to non-homogeneous film.

Acknowledgements

The authors would like to thank Mr. Junjiang Hu for refractive index and optical loss measurements.

References

- [1] O. Martins, J. Xu, R.M. Almeida, *J. Non-Cryst. Solids* 256–257 (1999) 25.
- [2] C. Urlacher, O. Marty, J.C. Plenet, J. Serughetti, J. Mugnier, *Thin Solid Films* 349 (1999) 61.
- [3] L. Lou, D. Boyer, G.B. Chadeyron, E. Bernstein, R. Mahiou, J. Mugnier, *Opt. Mater.* 15 (2000) 1.
- [4] L. Lou, W. Zhang, A. Brioude, C.L. Luyer, J. Mugnier, *Opt. Mater.* 18 (2001) 331.
- [5] G.K. Singh, V.K. Sharma, A. Kapoor, K.N. Tripathi, *Opt. Laser Technol.* 33 (2001) 455.
- [6] M. Bahtat, J. Mugnier, L. Lou, J. Serughetti, *Sol–Gel Opt. II: SPIE* 1758 (1992) 173.
- [7] D.-G. Chen, B.G. Potter, J.H. Simmons, *J. Non-Cryst. Solids* 178 (1994) 135.
- [8] S. Pelli, G.C. Righini, A. Scaglione, M. Guglielmi, A. Martucci, *Opt. Mater.* 5 (1996) 119.
- [9] J.W. Zhai, L.Y. Zhang, X. Yao, S.N.B. Hodgson, *Surf. Coat. Technol.* 138 (2001) 135.
- [10] H. Schmidt, *J. Non-Cryst. Solids* 112 (1989) 419.
- [11] K.-H. Haas, S. Amberg-Schwab, K. Rose, G. Schottner, *Surf. Coat. Technol.* 111 (1999) 72.
- [12] S. Motakef, J.M. Boulton, G. Teowee, D.R. Uhlmann, B.J.J. Zelinski, *Sol–Gel Opt. II: SPIE* 1758 (1992) 432.
- [13] Y. Sorek, R. Reisfeld, *Appl. Phys. Lett.* 63 (1993) 3256.
- [14] W.X. Que, Z. Sun, Y. Zhou, Y.L. Lam, Y.C. Chan, C.H. Kam, *Thin Solid Films* 359 (2000) 177.
- [15] W.X. Que, Y. Zhou, Y.L. Lam, Y.C. Chan, C.H. Kam, *J. Sol–Gel Sci. Technol.* 20 (2001) 187.
- [16] S. Motakef, T. Suratwala, R.L. Roncone, J.M. Boulton, G. Teowee, G.F. Neilson, D.R. Uhlmann, *J. Non-Cryst. Solids* 178 (1994) 31.
- [17] G.R. Atkins, R.M. Krolikowska, A. Samoc, *J. Non-Cryst. Solids* 265 (2000) 210.
- [18] K.-H. Haas, H. Wolter, *Curr. Opin. Solid State Mater. Sci.* 4 (1999) 571.
- [19] R. Ulrich, R. Torge, *Appl. Opt.* 12 (1973) 2901.
- [20] R.M. Almeida, P. Morais, H.C. Vasconcelos, B.S. Dunn, J.D. Mackenzie, E.J.A. Pope, H.K. Schmidt, M. Yamane, *Sol–Gel Opt. IV: SPIE* 3136 (1997) 296.
- [21] P. Innocenzi, A. Martucci, M. Guglielmi, L. Armelao, S. Pelli, G.C. Righini, G.C. Battaglin, *J. Non-Cryst. Solids* 259 (1999) 182.
- [22] W.X. Que, Y. Zhou, Y.L. Lam, Y.C. Chan, C.H. Kam, *Thin Solid Films* 358 (2000) 16.
- [23] M. Zevin, R. Reisfeld, *Opt. Mater.* 8 (1997) 37.
- [24] H.S. Gu, D.H. Bao, S.M. Wang, D.F. Gao, A.X. Kuang, X.J. Li, *Thin Solid Films* 283 (1996) 81.
- [25] X.G. Tang, Q.F. Zhou, J.X. Zhang, *Thin Solid Films* 375 (2000) 159.
- [26] C.V. Ramana, O.M. Hussain, B.S. Naidu, P.J. Reddy, *Thin Solid Films* 305 (1997) 219.
- [27] I. Mikulskas, E. Bernstein, J.C. Plenet, C. Bovier, R. Tomasiunas, V. Grivickas, J.V. Vaitkus, J. Mugnier, J. Dumas, *Mater. Sci. Eng. B69–70* (2000) 418.